

# Modeling and Simulation of Discontinua

**Session Organizer:** Shang-Hsien HSIEH (National Taiwan University)

## **Keynote Lecture**

The roots of possible chaotic behavior in modeling and simulation of discontinua

Antonio MUNJIZA\* (*University of London*), T. CARNEY, E. KNIGHT, R.P. SWIFT, D. GREENING, D. STEEDMAN (*Los Alamos National Laboratory*)

Motion analysis of mixed polyhedral and ellipsoidal particles

Chung-Yue WANG\*, Jopan SHENG, Chih-Jung HUANG, Ming-Hong CHEN (*National Central University*)

A fluid-particle simulation for two-phase granular flow

Li-Pen WANG, Ying-Pao LIAO, Chuin-Shan CHEN\*, Fu-Ling YANG, Shang-Hsien HSIEH (*National Taiwan University*)

Discrete element simulation of a collision-rich solid-liquid flow using a liquid-modified contact model

Fu-Ling YANG\*, Wei-Tze CHANG, Shang-Hsien HSIEH, Chuin-Shan CHEN (*National Taiwan University*)

For multiple-author papers:

Contact author designated by \*

Presenting author designated by underscore

## The roots of possible chaotic behaviour in modelling and simulation of discontinua

A.MUNJIZA<sup>1</sup>, T.CARNEY<sup>2</sup>, E.KNIGHT<sup>2</sup>, R.P.SWIFT<sup>2</sup>, D.GREENING<sup>2</sup>, D.STEEDMAN<sup>2</sup>

<sup>1</sup>University of London, Mile End Road, E1 4NS London UK; a.munjiza@qmul.ac.uk

<sup>2</sup>Los Alamos National Laboratory

### Abstract

The roots of possible chaotic behaviour in simulation of discontinua are investigated. Examples of such behaviour are demonstrated through simulations comprising few thousand to several hundred thousand particles. Finally, the results of discontinua simulations are classified and guidance for selection of benchmark problems and validation is given

### 1. Introduction

The last two decades have witnessed an explosion in research activity in the field of discontinua. A whole range of simulation methods have been developed to such an extent that systems comprising billions of particles in both 2D and 3D have been attempted. These include molecular dynamics methods, discrete element methods [2], the combined finite discrete element method [1][5] and particle methods. Due to the exponential growth in hardware performance in the same period, these methods no longer require supercomputers and simulations comprising up to one hundred million particles have been attempted on a desktop PC. The result is that an increasing number of people are using the methods for an increasing range of problems [4].

In this context, the experimental validation of simulations together with the development of benchmark problems has gained importance [3]. The problem is that all methods of discontinua are highly nonlinear. For instance, in the case of the combined finite-discrete element method each body (discrete element) deforms, fractures, fragments and at the same time interacts with discrete elements in its vicinity. Thus, the average combined finite-discrete element simulation is highly nonlinear to the extent that it is in a state of permanent bifurcation. This is illustrated in Figure 1 where two discrete elements with sharp corners are moving towards each other with velocity  $v$ .

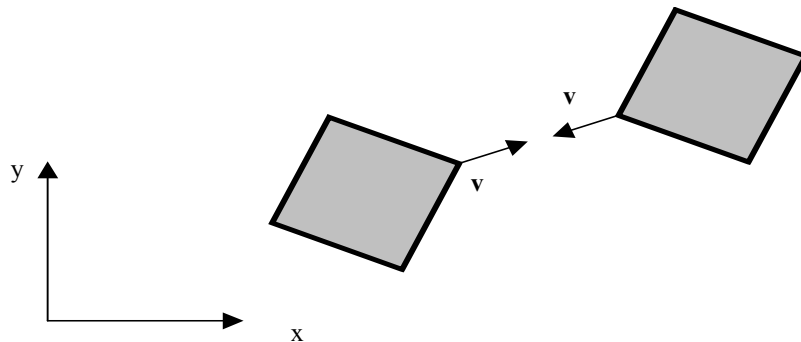


Figure 1: Two sharp corners approaching contact

If digital representation of the co-ordinates of all discrete elements and their velocity magnitude and velocity direction were exact, the discrete elements would simply bounce away from each other. Exact representation of

coordinates is not always possible not even in a theoretical sense and in such a case there can be three solutions to the above problem. If any coordinate of one of the above particles is say number  $\pi$ , all three solutions are equally probable regardless of the number of digits at which the CPU unit operates. In a system of discontinua comprising billions of particles, a large number of these bifurcation points are present at any time instance leading to sensitivity of discontinua simulations to the initial conditions. This sensitivity is similar in nature to what Edward Lorenz noticed while running computer models for weather forecasts in 1961 and can lead to what is termed deterministic chaos.

In this paper, the some reasons for loss of symmetry, sensitivity to initial conditions or possible chaotic behaviour of discontinua simulations are investigated through numerical experiments.

## 2. SELECTED EXAMPLES DEMONSTRATING LOSS OF SYMMETRY

In order to analyse the reasons behind the loss of symmetry in numerical simulations of discontinua, a beam shaped heap of closely packed particles of different shapes and sizes are assembled. The heaps are impacted by a rigid impacting body of triangular shape moving at initial velocity of 200 m/s. All the heaps considered are of the same shape and size; only the shape, size and number of identical particles making the heap is changing. There is no friction between particles.

**Heap TS.** This is a heap of small identical triangular particles. The particles are closely packed together in such a way that the left hand side of the heap is the mirror image of the right hand side of the heap. The motion sequence obtained using the discrete element method is shown in Figure 2. It can be observed that the symmetry is preserved to some extent in a sense that the left and right side look a mirror image of each other. However, by looking at the same results at higher magnification (Figure 3) it is evident that there exist quite a bit of local differences between the left and right side. This is especially noticeable if full screen movie is shown as will be done during the presentation.

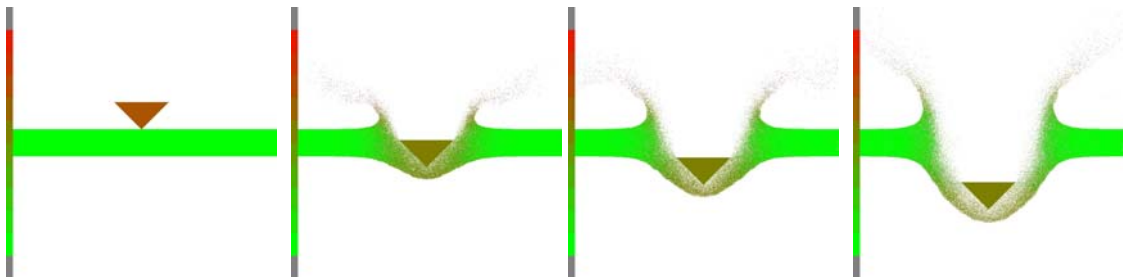


Figure 2 Motion sequence of a heap comprising 378 000 rigid triangles, low magnification

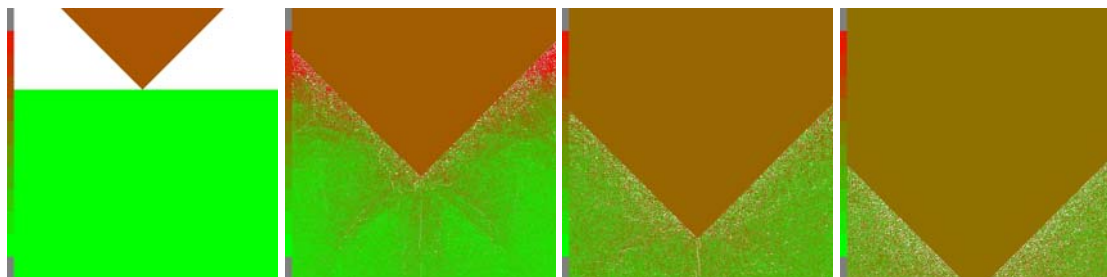


Figure 3 Motion sequence of a heap comprising 378 000 rigid triangles, high magnification

**Heap QL.** This is a heap of identical square shaped particles. The particles are closely packed together in such a way that the left hand side of the heap is the mirror image of the right hand side of the heap. The results of simulation (Figure 4) show quite “random” behaviour of especially top layer of the heap with particles seemingly randomly “springing” out. Closer observation using movies leads to the conclusion that as the layers of particles are pushed horizontally, the whole layer of particles buckles under axial force. This buckling is the main reason for the complex patterns of particle clusters observed. The same results shown at higher

magnification (Figure 5 and Figure 6) clearly demonstrate that not much symmetry is preserved at smaller length scales.

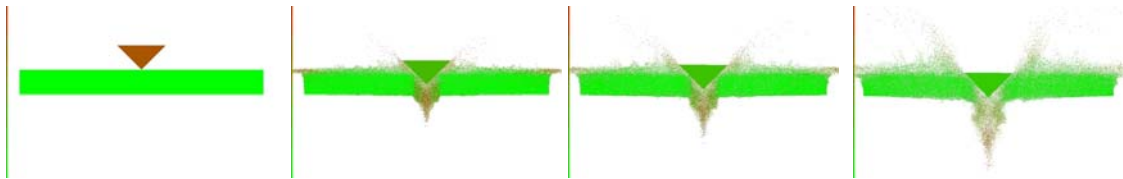


Figure 4 Motion sequence of a heap comprising 41k rigid quads

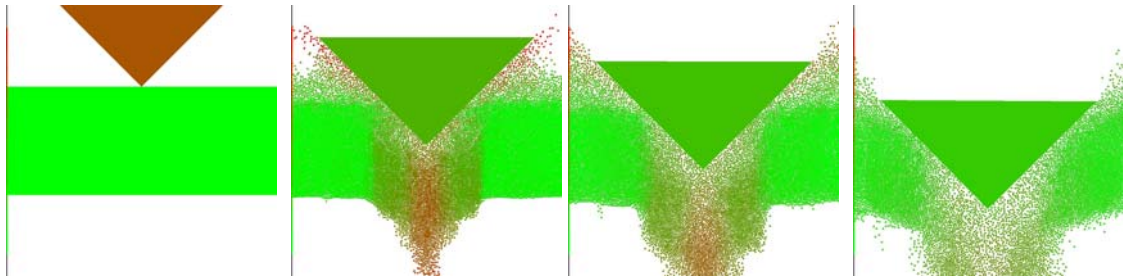


Figure 5 Motion sequence of a heap comprising 41k rigid quads, medium magnification

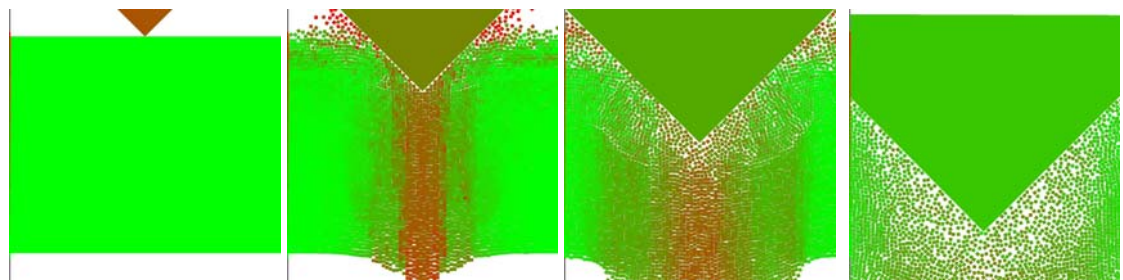


Figure 6 Motion sequence of a heap comprising 41k rigid quads, high magnification

**Heap HS.** This is a heap of identical hexagonal particles. The particles are closely packed together in such a way that the left hand side of the heap is the mirror image of the right hand side of the heap. The motion sequence obtained using the discrete element method is shown in Figure 7. Close inspection reveals a significant loss of symmetry with some similarities in “buckling patterns” as observed with square shaped particles, while the overall motion sequence to some extent resembles the motion sequence obtained using triangular particles. These clearly indicate that both buckling and corner to corner contacts are sources of bifurcation. Motion sequence shown at higher magnification (Figure 8) clearly demonstrates that the symmetry at this length scale has been completely lost.

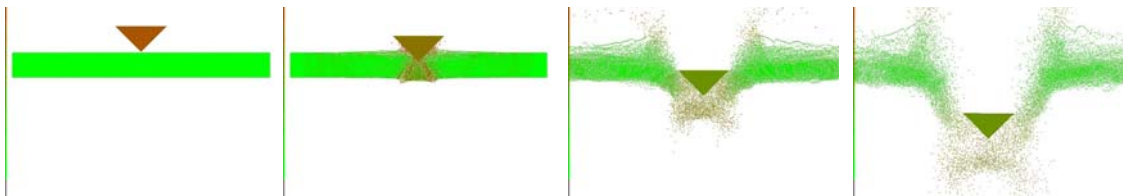


Figure 7 Motion sequence of a heap comprising 11k rigid hexes, low magnification

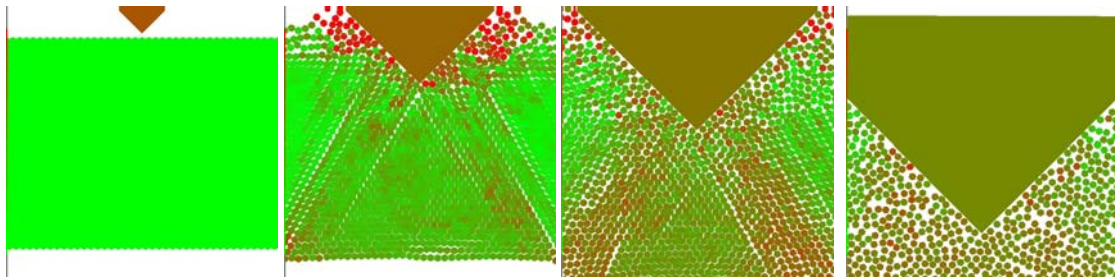


Figure 8 Motion sequence of a heap comprising 11k rigid hexes, high magnification

### 3. CONCLUSIONS

From the examples shown in the previous section, it is evident that the loss of symmetry, sensitivity to initial conditions and possibly chaotic behaviour is an integral part of numerical simulations involving discontinua. Micromechanical mechanisms observed include: (a) bifurcation instances such as corner to corner contact (for instance in the case of triangular heaps) (b) buckling of a stack of flat particles under combination of axial and inertia forces (for instance in the case of heaps made of square shaped particles) (c) combination of bifurcation instances and buckling (these are evident in the case of heaps made of hexagonal particles).

It is worth noting that in all examples shown in this paper the overall symmetry is to a large extent preserved. However, if one looks at the results at higher magnification, the loss of symmetry becomes more pronounced and at very high magnification hardly any symmetry can be observed. In other words, the results show that the loss of symmetry is more pronounced at lower length scales. The results shown in this paper are mostly of qualitative nature, nevertheless the results clearly demonstrate that the sensitivity to initial conditions, loss of symmetry and possible chaotic behaviour are not simply a numerical artefact (a result of for instance rounding errors). Sensitivity to initial condition, loss of symmetry and possible chaotic behaviour are very often an integral part of the nature of problems that the methods of the computational mechanics of discontinua aim at solving.

It is therefore important that both the developers of computational tools and practitioners using the software take into account these sensitivities when analysing the results or when verifying and validating numerical tools. This is especially true when choosing the benchmark problems. On the other hand, sensitivity to initial conditions should never be automatically assumed to be responsible for say loss of symmetry. This is because numerical noise, bad algorithms, unstable numerical solutions and coding bugs very often lead to the results that may be mistaken for sensitivity to initial conditions. Presence of loss of symmetry, sensitivity to initial conditions or chaotic behaviour should only be tolerated in the numerical simulation if they are the result of the nature of the problem and not merely the result of faulty software or faulty numerical methods.

By simply looking at still images, it is difficult to truly appreciate the real beauty of the phenomena demonstrated - thus, in the presentation the above examples will be shown using "virtual movies".

### References

- [1] Komodromos, P.I. & Williams, J.R. (2004), "Dynamic simulation of multiple deformable bodies using combined discrete and finite element methods". *Engineering Computations*, 21, 431-48.
- [2] Cundall, P.A. & Strack, O.D.L. (1979), "A discrete numerical model for granular assemblies." *Geotechnique*, 29, 47-65.
- [3] Li, Y., Xu, Y. & Thornton, C. (2005), "A comparison of discrete element simulations and experiments for 'sandpiles' composed of spherical particles". *Powder Technology*, 160, 219-228.
- [4] Cleary, P.W., Morisson, R. & Morrell, S. (2003), "Comparison of DEM and experiment for a scale model SAG mill". *International Journal of Mineral Processing*, 68, 129-165.
- [5] Munjiza, A. (2004), *The Combined Finite-Discrete Element Method*, John Wiley & Sons.

## Motion analysis of mixed polyhedral and ellipsoidal particles

Chung-Yue WANG\*, Jopan SHENG, Chih- Jung HUANG, Ming-Hong CHEN

Department of Civil Engineering, National Central University  
Chungli, 32001, Taiwan, ROC  
cywang@cc.ncu.edu.tw

### Abstract

In this paper, a new algorithm and a computer code are developed for the motion analysis of a system composed of mixed polyhedral and ellipsoidal particles. In this algorithm, we categorize the complicated contact behavior into three types as (1) ellipsoid to the ellipsoid, (2) ellipsoid to Polyhedron, (3) polyhedron to polyhedron. In addition, the contact analysis algorithm is constituted by several kinds of detail classification to accelerate the speed of simulation. The mass moment of inertia tensor of a polyhedron is calculated by a simplex integration technique. The ellipsoid is approximated by a revolution of a four-arc ellipse. The normal and shear contact forces among particles are calculated through contact spring models. Before conducting analysis of systems containing many particles, the accuracy of this code is verified by some standard testing problem of rigid body dynamics. Some packing configurations and motion analyses of mixed particles generated by this code are demonstrated.

### 1. Introduction

The number of processes involving solids in the chemical, petrochemical, pharmaceutical, biochemical, food industry, civil engineering as well as in energy conversion and environmental processes is such that a high percentage of the research activity is concerned with motion analysis of solids. The motion of discrete solids presents different characteristics depending on the type of system, solid concentration, arrangement, shape, cohesion and interactions. Although large sets of experimental data were available today on diverse granular and multi-phase flows, a proper discussion and understanding of the involved phenomena cannot be attained without the help of numerical simulations (Di Renzo et al. [1]). A typical technique for the numerical simulation of granular medium is the distinct element method (DEM) (Cundall and Strack [2]). The basic idea behind the DEM is based on the law of mechanics: the trajectory of each particle is calculated, considering all the forces acting on it and integrating the Newton's second law, the Euler's equation of motion and the kinematic equations for position and orientation. DEM has been applied widely in simulating and predicting the performances of many processes involving granular solids. In the analysis of DEM, the contact detection and the calculation of interaction forces among particles are the core processes. The nature of these interactions is determined by particle size, shape, density, friction angle, cohesion and other properties. These tasks will be complicated by the consideration of the nonlinear material properties and the nonspherical geometrical shapes of particles in the granular assemblies.

Few literatures can be found on the motion analysis of three-dimensional nonspherical particles using DEM. In the past decade, some researchers have used ellipsoidal solids in DEM computations (Lin and Ng [3, 4], Quadfel and Rothenburg [5]). Several investigators have developed other 3D composite nonspherical particles that are entirely composed of overlapping spheres or spherical pieces (Favier et al. [6, 7]), but these multisphere composites are neither smooth nor convex. An ovoid shape was first developed by the first author of the present paper (Wang et al. [8]) and a general ovoid shape for both oblate and prolate particles was introduced by Kuhn [9] later. On the motion analysis of polyhedral particles, Cundall [10, 11] proposed a common plane method (CPM) and implemented in the DEM program 3DEC for the system composed of many polyhedral blocks. Nezami et al [12, 13] proposed an improved version of CPM called fast common plane method (FCP) and the

shortest link method (SLM) to reduce the searching time of common plane. Zhao et al. [14] developed a three-dimensional discrete element code (BLOKS3D) for efficient simulation of polyhedral particles of any size.

In the present paper, we focus on the problem of the contact detection of assemblies composed of mixed ellipsoidal and polyhedral particles.

## 2. Calculations of Particle Properties and Contact Detection Algorithms

To develop a discrete element code, the calculation of particle properties as the mass and mass moment of inertia and the contact detection algorithms among particles are the main part of the analysis. In the following sections, these subjects for the system composed of mixed ellipsoidal and polyhedral particles will be roughly explained.

### 2.1 Motion Analysis of Ellipsoidal Particles

To simplify the contact detection analysis of two ellipsoids in space, Wang et al. [8] have first developed an algorithm of contact detection for prolate and oblate particles generated by the revolution of 4-arc ellipses as shown in Fig. 1. Spherical surfaces are formed by the revolution of arcs FG, HE in Fig. 1(a) and by the arcs EF, GH in Fig. 1(c). Torus surfaces are formed by the revolution of arcs HG, EF in Fig. 1(a) and by the arcs FG, HE in Fig. 1(c). In this algorithm, the contact type of sphere-to-sphere, torus-to-torus and sphere-to-torus have to be examined. Detail contact theories and the calculation of the volume and moments of inertias of this kind of 3D particles can be found in the work done by Kuhn [9]. Contact force is calculated by the multiplication of the penetration depth and the contact spring stiffness. A code has been developed by the authors to conduct the motion analysis of ellipsoidal particles in space.

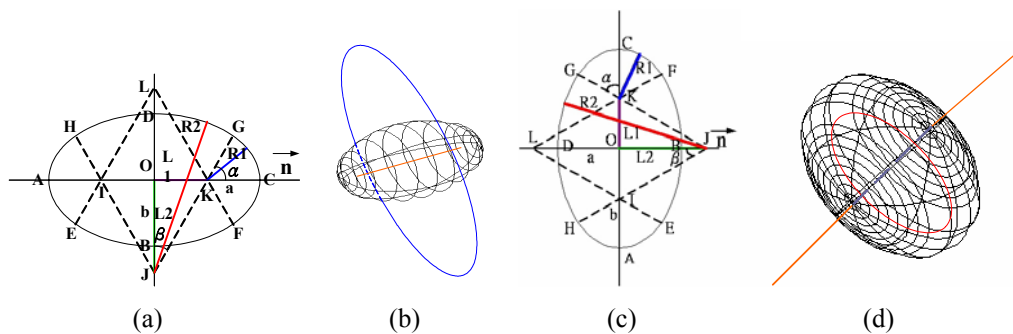


Figure 1: Prolate ovoid and oblate ovoid formed by the revolution of 4-arc ellipses

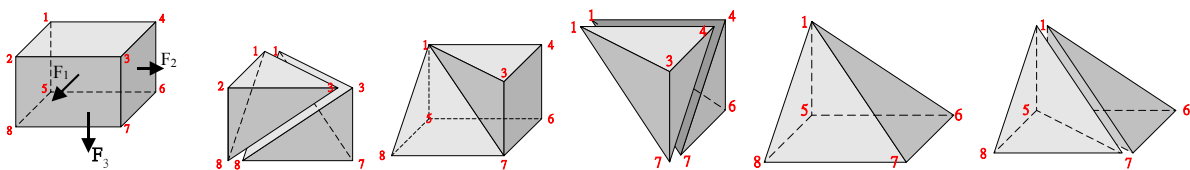


Figure 2: Decomposition of a cube into a less number of tetrahedrons by a cutting process by linking vertex 1 with triangles on face  $F_1$ ,  $F_2$  and  $F_3$ .

### 2.2 Motion Analysis of Polyhedral Blocks

An algorithm and a computer code have been developed by the authors (Sheng et al. [15]) developed for numerical simulations of a system composed of polyhedron of any shape, which can undergo arbitrary large motions and rotations. A cutting process was developed to decompose any polyhedron into a less number of tetrahedrons. As shown in Fig. 2, a cube is decomposed by the vertex 1 and triangles on faces  $F_1$ ,  $F_2$  and  $F_3$ ; those are not in the same plane with vertex 1. The volume and the tensor of the mass moment of inertia of each tetrahedron respect to the global coordinates can be calculated by the simplex integration developed by Shi [16]. Then the parallel theorem is used to determine the tensor of the mass moment of inertia of the polyhedron

respect to its centroid. In the motion analysis of polyhedral blocks, only contact types of vertex-to-face and edge-to-edge are required for contact detection, although six types of contacts are possible between any two polyhedral blocks as shown in Fig. 3. It is noted that, the vertex-to-face contact and the edge-to-edge contact are the fundamental modes of the other four contact types. In addition, the contact system is decomposed into contact detection hierarchies to accelerate the simulation speed. The mutual reactions among elements are taken account by the relative forces and contact through normal and tangential spring model.

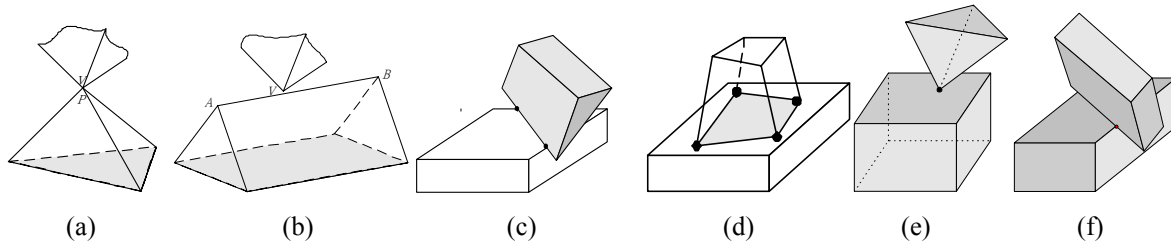


Figure 3: (a) vertex-to-vertex contact, (b) vertex-to-edge contact, (c) edge-to-face contact, (d) face-to-face contact (e) vertex-to-face contact, (f) edge-to-edge contact.

### 2.3 Motion Analysis of Mixed Ellipsoidal and Polyhedral Particles

In the motion analysis of a particle assemblies composed of ellipsoids and polyhedrons, the contact analysis between ellipsoid and polyhedron is another task. There are three contact types: vertex-to-ellipsoid contact, edge-to-ellipsoid and face-to-ellipsoid between these two kinds of particles. The detections of the first two types of contact are standard features of coding. While the contact between an ellipsoid and a face of polyhedron is further evaluated by which section of the ovoid contacts the polyhedral face. As shown in Fig. 4 (b), if the angle  $\theta$  between the revolution axis  $\vec{n}$  and the normal vector  $\vec{N}$  of the face is larger than the half range angle  $\alpha$  of spherical section, the torus section of the ovoid may contact the polyhedral face. Furthermore, If the extreme distance between the point A on an outer ring of the torus section and the point P on face is less than the radius  $r_2$  of the torus surface, then the point P is the contact point of the torus section of the ovoid with the polyhedron. If the angle  $\theta$  is less than the angle  $\alpha$ , then the spherical section of the avoid may contact the polyhedral face. It contacts the face when the distance between the centroid and the face is less than the radius  $r_1$  of the spherical section. Figure 5 shows the motion analysis of mixed ellipsoidal and polyhedral particles conducted by the code developed based on the aforementioned theories.

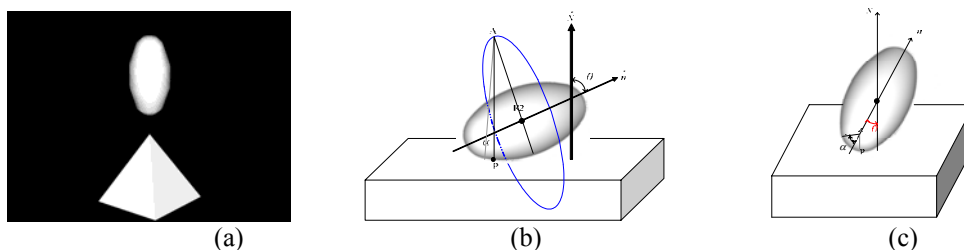


Figure 4: (a) vertex-to- ellipsoid contact, (b) contact between torus section of an ovoid and plane, (c) contact between spherical section of an ovoid and plane.

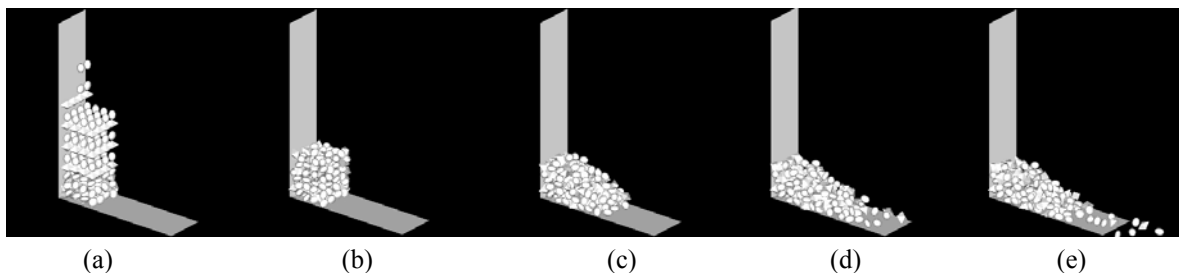


Figure 5: Motion analysis of mixed ellipsoidal and polyhedral particles.

### 3. Discussion and Conclusions

The distinct element method (DEM) has proven to be effective in characterizing the behavior of particles in granular flow simulation. This paper presents a simulation algorithm for the motion analysis of medium composed of mixed ellipsoidal and polyhedron particles. It describes an effort to enhance the available algorithms and further the engineering application of DEM. Contact detection of the complex geometrical configuration at any time is the main part of the presented paper. However, the modeling of the collision process between particles is critical to the accuracy of simulation. It should be well investigated in the future.

### References

- [1] Di Renzo A, Di Maio FP. Comparison of contact-force models for the simulation of collisions in DEM-based granular flow codes. *Chemical Engineering Science* 2003; 525–541.
- [2] Cundall PA, Strack ODL. A discrete numerical model for granular assemblies. *Geotechnique* 1979; 29:47-65.
- [3] Lin X, Ng TT. Contact detection algorithms for three-dimensional ellipsoids in discrete element modeling. *International Journal for Numerical and Analytical Methods in Geomechanics* 1995; 19; 9: 653-659.
- [4] Lin X, Ng TT. A three-dimensional discrete element model using arrays of ellipsoids. *Geotechnique* 1997; 47; 2:319-329.
- [5] Quadfel H, Rothenburg L. An algorithm for detecting inter-ellipsoid contacts. *Comp. Geotechn.* 1999; 24; 4: 245-263.
- [6] Favier JF, Abbaspour-Fard MH, Kremmer M, Raji AO. Shape representation of axi-symmetrical, non-spherical particles in discrete element simulation using multi-element model particles. *Engineering Computations* 1999; Vol. 16 No. 4; 469-480.
- [7] Favier JF, Abbaspour-Fard MH, Kremmer M. Modeling nonspherical particles using multisphere discrete elements. *Journal of Engineering Mechanics* 2001; 127; 10: 971-977.
- [8] Wang CY, Wang CF and Sheng J. A Packing Generation Scheme for the Granular Assemblies with 3D Ellipsoidal Particles. *International Journal for Numerical and Analytical Methods in Geomechanics* 1999; 23: 815-828.
- [9] Kuhn MR. Smooth convex three-dimensional particle for the discrete-element method. *Journal of Engineering Mechanics* 2003; 129; 5:539-547.
- [10] Cundall PA. Formulation of a three-dimensional distinct element model-Part I: a scheme to detect and present contacts in a system composed of many polyhedral blocks. *Int. J. of Rock Mech., Min. Sci. & Geomech. Abstr.* 1988a; 25;3:107-116.
- [11] Cundall PA. Formulation of a three-dimensional distinct element model-Part II: mechanical calculations for motion and interaction of a system composed of many polyhedral blocks. *Int. J. of Rock Mech., Min. Sci. & Geomech. Abstr.* 1988b; 25;3:107-116.
- [12] Nezami E, Hashash YMA, Zhao D, Ghaboussi J. A fast contact detection algorithm for 3D discrete element method. *Computers and Geotechnics* 2004; 31: 575-587.
- [13] Nezami E, Hashash YMA, Zhao D, Ghaboussi J. Shortest link method for contact detection in discrete element method. *International Journal for Numerical and Analytical Methods in Geomechanics* 2006; 30; 8: 783-801.
- [14] Zhao D, Nezami EG, Hashash YMA, Ghaboussi J. Three-dimensional discrete element simulation for granular materials, *Engineering Computations: International Journal for Computer-Aided Engineering and Software* 2006; .23:749-770.
- [15] Sheng J, Hsu HC, Wang CY. Motion Analysis for System Composed of Polyhedral Blocks. *Journal of the Chinese Institute of Civil and Hydraulic Engineering* 2002. 14; 4: 603-613. (in Chinese)
- [16] Shi GH. Modeling Dynamic Rock Failure by Discontinuous Deformation Analysis with Simplex Integrations. *Geotechnical Lab., U.S. Army Engineer Waterways Experiment Station, Viskburg, MS.* 1995: 39180-6199.

## A fluid-particle simulation for two-phase granular flow

Li-Pen WANG\*, Ying-Pao LIAO\*, Chuin-Shan CHEN\*, Fu-Ling YANG†, and Shang-Hsien HSIEH\*

\*Dept. of Civil Engineering, National Taiwan University, Taipei, Taiwan (fangwlp@caece.net)

†Dept. of Mechanical Engineering, National Taiwan University, Taipei, Taiwan

### Abstract

A fluid-particle simulation scheme is formulated for two-phase granular flows by integrating the discrete element method (DEM), the Navier-Stokes equation solver, and the immersed boundary method. The theoretical challenge of this scheme is twofold. First, an efficient algorithm is required to calculate the boundary forces exerted by the fluid over the particle surface to advance the particle motion. A subsequent calculation should follow to consider how the moving surface modifies the surrounding liquid motion. To handle this strongly coupled solid-liquid interaction, a novel algorithm—based on the immersed boundary method (IBM)—is formulated. The obtained interaction force is then integrated with a DEM and a Navier-Stokes equation solver, SIMPLE, to update the solid and the fluid motion. This hybrid scheme shall be useful for two-phase flow problems with many particles and strong solid-liquid interactions.

### 1. Introduction

The motion of a solid-plus-liquid two-phase granular flow has been studied at both the microscopic (particle size) and the macroscopic level (flow size) via laboratory experiments and numerical simulations. Despite the advance of experimental techniques, detailed measurements on the solid-liquid interaction force has only been achieved at steady-state. The flow complexity poses a great challenge to the experimentalists to monitor the solid-liquid interaction during an unsteady process. Thus, numerical simulation serves as an alternative, but yet powerful, means to investigate the particle-level solid-liquid interactions. The microscopic mechanics can be further integrated to obtain information of the unsteady bulk dynamics. Though there exists an extensive literature on the subject of computational fluid dynamic (CFD), it is an expensive task to calculate the frequent and intrinsically unsteady solid-liquid interaction with most of the traditional schemes. Thus, a hybrid scheme is attempted in this work by exploiting the advantages of various numerical methods to simulate different components that determine a two-phase granular flow. A discrete element method (DEM) will be adopted to advance the individual particles, after a total hydrodynamic force is calculated from an immersed boundary method (IBM). The IBM is coupled with the surrounding liquid motion which will be solved using SIMPLE, a well-developed CFD solver for the full Navier-Stokes equation. An algorithm is proposed as follows to integrate these numerical schemes in order to investigate the interplay between the particles and the surrounding fluid.

### 2. A two-phase model simulation scheme

The proposed algorithm is inspired by *Proteus*—a direct numerical method for particulate flow simulation that combines IBM, the direct forcing method and the lattice Boltzmann method (LBM) (Feng and Michaelides [2]). The procedures are illustrated in Figure 1. The calculated flow fields, the particle position and velocity from the previous time step,  $\mathbf{u}^n$ ,  $\mathbf{X}^{p(n)}$ , and  $\mathbf{U}^{p(n)}$ , are used to calculate the total hydrodynamic force acting on the solid particle,  $\mathbf{F}^n$ . The subsequent particle position and velocity,  $\mathbf{X}^{p(n+1)}$  and  $\mathbf{U}^{p(n+1)}$ , is updated using DEM. The predicted particle motion imposes a new boundary condition on the flow field. Thus, the surrounding liquid

motion, governed by the full Navier-Stokes equation in Eq(1), will be solved until the new boundary conditions are met at the solid surface, i.e. the  $\mathbf{X}^{\mathbf{P}(n+1)}$  and  $\mathbf{U}^{\mathbf{P}(n+1)}$ .

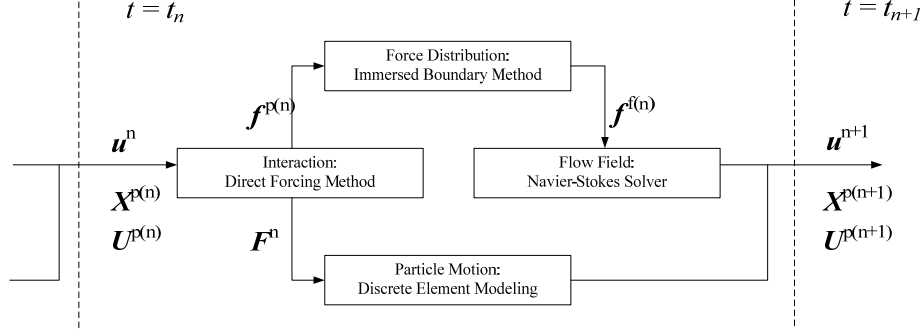


Figure 1: The procedures of the proposed simulation scheme.

At each time step, the motion of an incompressible and viscous (Newtonian) fluid is governed by the Navier-Stokes equation:

$$\nabla \cdot \mathbf{u} = 0, \text{ and } \rho \left( \frac{\partial \mathbf{u}}{\partial t} + \mathbf{u} \cdot \nabla \mathbf{u} \right) = \mu \nabla^2 \mathbf{u} - \nabla p + \mathbf{f}, \quad (1)$$

where  $\mathbf{u}$  is the fluid velocity,  $p$  is the thermodynamic pressure, and  $\rho$  and  $\mu$  denote the fluid density and viscosity respectively. The external force,  $\mathbf{f}$ , includes gravity and a component,  $\mathbf{f}^{f(n)}$ , resulted from the solid-liquid interaction. A well-developed solver for (1)—SIMPLE—is adopted in the current work and is briefed in 3.1. The two solvers, DEM and SIMPLE, are connected in the current scheme when the solid-liquid interaction force,  $\mathbf{F}^n$  and  $\mathbf{f}$ , are calculated.

## 2.1 The solid-liquid interaction force

Since Eq(1) is also valid for the points located at the particle surface, the fluid body force at each Eulerian grid point (density) can be readily obtained with an discrete form:

$$f_i = \rho \left( \frac{u_i^n - u_i^{n-1}}{\Delta t} + u_j^{n-1} u_{j,i}^{n-1} \right) - \mu u_{i,jj}^{n-1} + p_{,i}^{n-1}. \quad (2)$$

By imposing the no-slip boundary condition at the particle solid surface,  $\mathbf{u}^n = \mathbf{U}^{\mathbf{P}(n)}$  on the surface Lagrangian grid points. Thus, the fluid body force on the particle surface,  $\mathbf{f}^{\mathbf{P}(n)}$ , can be estimated by :

$$f_i^{\mathbf{P}(n)} = \rho \left( \frac{U_i^{\mathbf{P}(n)} - u_i^{n-1}}{\Delta t} + u_j^{n-1} u_{j,i}^{n-1} \right) - \mu u_{i,jj}^{n-1} + p_{,i}^{n-1}, \quad (3)$$

To obtain the fluid body force,  $\mathbf{f}^{f(n)}$ , required as an input in SIMPLE, the IBM is employed to distribute the particle surface force,  $\mathbf{F}(s,t)$ , over the interface—the immersed boundary  $\Gamma$  (Feng & Michaelides [2]; Peskin [4]):

$$\mathbf{f}(\mathbf{x}, t) = \int_{\Gamma} \mathbf{F}^n(s, t) \delta(\mathbf{x}(t) - \mathbf{X}(s, t)) ds. \quad (4)$$

The spread function  $\delta(\cdot)$  is used to distribute the nodal surface force—on a Lagrangian node  $\mathbf{X}(s,t)$  described by the Lagrangian parametric coordinate  $s$  along the surface  $\Gamma$ —to the adjacent Eulerian fluid nodes  $\mathbf{x}(t)$ . By integrating Eq(4) over a small Eulerian area  $\varepsilon$  that covers  $\Gamma$ , we refine the IBM relation between the fluid body force and the immersed boundary force for the interaction force density as:

$$\int_{\varepsilon} \mathbf{f}(\mathbf{X}(s,t)) dA = \mathbf{f}^{P(n)}(\mathbf{X}(s,t)) \varepsilon = \int_{\Gamma} \mathbf{F}^n(s,t) \left( \int_{\varepsilon} \delta(\mathbf{x} - \mathbf{X}(s,t)) dA \right) ds = \int_{\Gamma_{\varepsilon}} \mathbf{F}^n(s,t) ds. \quad (5)$$

In Eq(5),  $\varepsilon$  is the influence area between the adjacent Eulerian nodes and the Lagrangian node at  $s$  and  $\Gamma_{\varepsilon}$  is the intersection of  $\varepsilon$  and the particle boundary  $\Gamma$ . Through Eq(5), we may estimate the total force exerted on the particle by the surrounding liquid by a direct surface intergraion of  $\mathbf{F}^n$  as  $\mathbf{F} = \int_{\Gamma} \mathbf{F}^n(s,t) ds$ , required for the following DEM calculation; the corresponding force exerted on the surrounding Eulerian nodes,  $\mathbf{f}^{f(n)}$ , can also be calculated through the spreading process of Eq(4).

## 2.2 Numerical method for solving particle and the fluid motion: DEM and SIMPLE algorithm

The discrete element model adopted in this study has been well developed based on a flexible in-house C++ framework, VEDO (VERSatile Discrete Objects framework) and has been verified and applied in many studies (Chang and Hsieh [1]). As for the fluid motion, a Semi-Implicit Method for Pressure-Linked Equations (SIMPLE), developed by Patankar and Spalding (Tannehill, *et al.* [5]) in 1972, is developed herein as a Navier-Stokes solver. The procedure is based on an iterative process of guess-and-correct operations on solving the momentum equation which procedure is constrained by the continuity equation in the Navier-Stokes equations. Figure 2(a) demostrantes SIMPLE procedures in which the pressure corection equation is the most time-consuming step. To suppress this computational cost for a future simulation with many particles, this work employs a SParse Object Oriented Linear Equations Solver (SPOOLES 2.2—a C library for solving sparse real and complex linear systems of equations) to compute the pressure correction term.

## 3. Preliminary results

To verify the recently implemented SIMPLE algorithm, a benchmark problem for 2D Navier-Stokes equations—a 2D cavity flow—is chosen. The preliminary results are presented and discussed in the following. The development of the immersed boundary method is underway. As depicted in Figure 2(b), an incompressible and viscous liquid in a square solid domain ( $D \times D$ ) is driven by an upper lid flow that moves at a constant horizontal velocity,  $U_0$ .

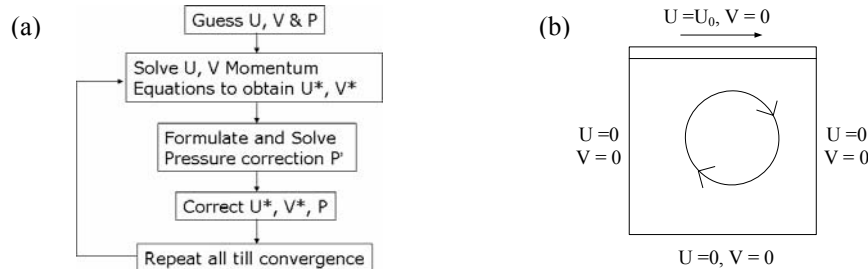


Figure 2: (a) The procedures of SIMPLE algorithm; (b) Driven cavity flow in a square domain.

A uniform 100x100 computation grid is used in this simulation and the resulting velocity profile is compared to the literature in Figures 3 and 4 at different Reynolds numbers,  $Re = \rho U_0 D / \mu$ , which characterizes the inertial and the viscous forces on a flowing fluid. The streamline for the flows at  $Re = 400$  and  $Re = 1,000$  is plotted in Figures 3(a) and 4(a) respectively. A primary vortex is developed across the whole cavity. A secondary vortex can be found at the right-bottom corner while a third, but smaller, vortex is developed at the left-bottom corner. At higher  $Re$ , the liquid moves at a greater inertial force which can ‘push’ the primary vortex further into the cavity. In figures 3(b), (c) and 4(b), (c), the horizontal and the vertical components of the liquid velocity, ( $u$ ,  $v$ ), are plotted along the center vertical and horizontal lines. To examine the performance of the SIMPLE algorithm, our results are compared to the reference solution, obtained by Vorticity-Stream Function approach (Ghia, *et al.* [3]) and good agreement validates the SIMPLE NS solver.

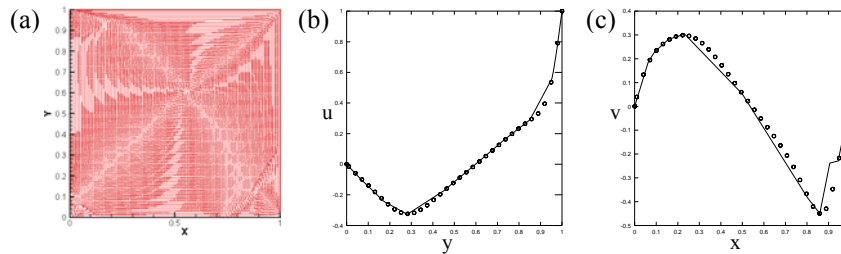


Figure 3: Re = 400 (a) streamline, (b) u-velocity, and (c) v-velocity

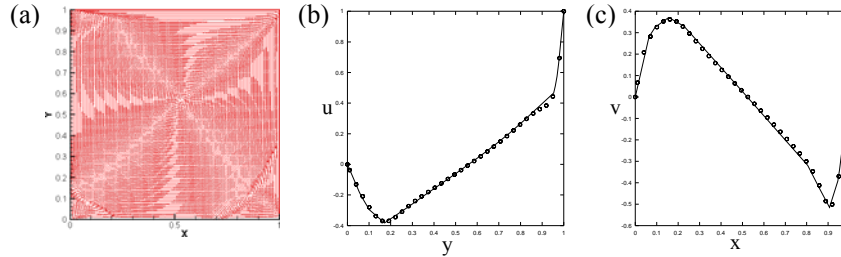


Figure 4: Re = 1000 (a) streamline, (b) u-velocity, and (c) v-velocity

#### 4. Summary and prospective future work

In this paper, an integrated numerical scheme is presented for the computation of a two-phase granular with many particles and strong solid-liquid interaction. It combines the discrete element method for the solid particle motion and a solver for the Navier-Stokes equation that governs the fluid motion. The two schemes are coupled by the solid-liquid interaction force, which is calculated at an intermediate step using an algorithm based on the immersed boundary method. SIMPLE, as the Navier-Stokes equation solver, has been implemented successfully. The development of immersed boundary method for the solid-liquid interaction force is underway, from which, we aim to simulate the motion of one to two interacting particles with a viscous surrounding. The integrated scheme proposed herein shall be useful for the future simulations of a fluid flow with many particles, which will be a powerful means to study the bulk behavior, both steady and unsteady, of a solid-liquid two-phase granular flow.

#### Acknowledgement

We are thankful to Dr. C. L. Chiu (Hydrotech Research Institute of National Taiwan University) for insightful discussions on the simulation of fluid motion. This research was supported by the Excellent Research Projects at National Taiwan University.

#### Reference

- [1] Chang WT and Hsieh SH. Parametric study on three dimensional discrete element simulation of self-compacting concrete mortar flow behaviour. *Proceedings of the 19<sup>th</sup> KKCNN Symposium on Civil Engineering*. 197-200, Kyoto, Japan, December, 2006.
- [2] Feng ZG and Michaelides EE. *Proteus*: a direct forcing method in the simulations of particulate flows. *Journal of Computational Physics* 2005; **202**: 20-51
- [3] Ghia, U, Ghia KN, Shin CT. High-Re solutions for incompressible flow using the Navier-Stokes equations and a multigrid method. *Journal of Computational Physics* 1982; **48**:387-411.
- [4] Peskin, CS. The immersed boundary method. *Acta Numerica* 2002; **11**:479-517
- [5] Tannehill JC, Anderson DA, Pletcher RH. *Computational Fluid Mechanics and Heat Transfer* (2nd edn). Taylor & Francis, 1997.

## Discrete element simulation of a collision-rich solid-liquid flow using a liquid-modified contact model

Fu-Ling YANG\*, Wei-Tze CHANG†, Shang-Hsien HSIEH†, and Chuin-Shan CHEN†

\*Dept. of Mechanical Engineering, National Taiwan University, Taipei, Taiwan ([fulingyang@ntu.edu.tw](mailto:fulingyang@ntu.edu.tw))

†Dept. of Civil Engineering, National Taiwan University, Taipei, Taiwan

### Abstract

This work presents how a discrete element method (DEM) can be exploited to calculate the bulk motion of a solid-liquid mixture with significant liquid effects. Without the interstitial fluids, a traditional DEM scheme often employs a hard-sphere or soft-sphere model to describe direct particle interactions. Contact model parameters, such as the spring and the damping constants or the coefficient of restitution and the friction coefficient, depend on the particle properties and are often assumed constant. With interstitial liquid, however, the contact mechanisms between dry surfaces can change greatly by liquid incompressibility and viscosity. A recently developed 'wet collision model', characterizing the liquid viscous damping and lubricating effects, is incorporated into a DEM scheme. With liquid-modified model parameters, the "dry grains with wet collision" DEM scheme is applied to simulate an unsteady wet granular flow with frequent particle collisions. The proposed methodology preserves the computational efficiency of DEM and considers liquid effects on a physical ground. The particle-level information from DEM can be averaged to reveal the physics of solid-liquid flows. To evaluate and validate the current scheme, the computational results will be further compared to available experimental data.

### 1. Introduction

In a wet granular flow, a solid-plus-liquid flow in which the two components move with comparable inertia, the strong interactions between the heterogeneous constituents introduce new mechanisms for momentum transport and energy dissipation in the bulk. With liquid-modified 'microscopic' mechanics at particle level, a 'macroscopic' mixture behavior may deviate from that of a dry bulk. The rheology of solid-liquid flows comprises an active field of research due to their prevalence in both natural and industrial fields. Our understanding of their behavior, however, is still fragmental due to difficult experimental instrumentations and un-unified theoretical approaches. Though computational approach has gained much potential as a research means with the fast-growing computational power, progress in simulating an unsteady solid-liquid flow has been somewhat limited. The main difficulty resides in the random and frequent particle motion that poses a complicate boundary condition beyond the scope of traditional CFD schemes. Thus, the current approach avoids the expensive simulation on the solid-liquid interaction force, but accounts for the liquid effects on two colliding particles in a soft-sphere contact model with modified parameters.

### 2. Wet collision model and the liquid-modified DEM scheme

#### 2.1 Wet collision model

In Yang and Hunt [1], systematic experimental investigations were conducted for collisions between two solid spheres in an incompressible and viscous liquid. A wet coefficient of resitution,  $e_{wet}$ , was defined to characterize the kinetic energy loss in one collision. This parameter is found well correlated with the particle Stokes number,  $St_B$ , as shown in figure 1 where the parameters are defined. Since the  $e_{wet}-St_B$  relation collapses to that measured for immersed particle-wall collisions (presented with☆; Joseph *et al.*[2]), a fitted relation that uses only particle-wall data is adopted,  $e_{wet} = e_{dry} \exp[-35/St_B]$  (Legendre *et al.*[3]), to predict a liquid-modified  $e_{wet}$  in this work.

The liquid-lubricated friction coefficient,  $f = 0.01$  between glass surfaces (Joseph *et al.*[2]), is adopted for the spheres used in the laboratory experiments.

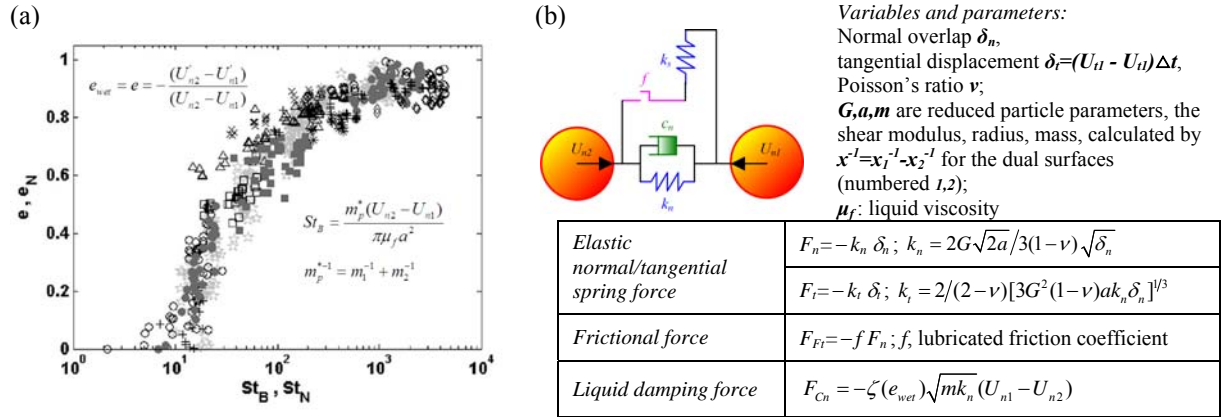


Figure 1: (a) The wet coefficient of restitution as a function of particle Stokes number (b) The soft-sphere contact model and working formulas (Mindlin and Deresiewicz [4]; Cundall [5])

## 2.2 DEM scheme with the wet collision model

The current soft-sphere contact model is depicted in figure 1(b), in which the collision-induced force on the two particles is decomposed into three components along or tangent to the contact normal, defined by the line of centers when two spheres are in contact. The three forces include: (1) an *elastic force* due to surface deformation that affects the total contact duration but does not dissipate kinetic energy, (2) a *frictional force* that accounts for energy loss in tangential sliding, and (3) a *liquid damping force* that depends on the relative normal velocity between the surfaces and is modeled with a normal dashpot.

The normal and tangential elastic forces are described by two springs along and perpendicular to the contact normal. The respective stiffness,  $k_n$  and  $k_t$ , required for force calculation depend on the elastic properties, the geometry of the particles, and an overlap predicted for un-deformed surfaces before contact (Mindlin and Deresiewicz [4]; Cundall [5]). The frictional force is assumed to be of Coulomb type, which depends on a lubricated friction coefficient,  $f$ , and the normal elastic deformation force. To account for the kinetic energy loss due to normal surface motion, a normal dashpot is implemented giving rise to a deformation-rate dependent force. For its dissipating nature, the damping coefficient,  $\zeta$ , shall be related to the coefficient of restitution. While different models have been proposed for  $\zeta - e_{dry}$  correlations for dry collisions beyond elastic regime, a linear model,  $\zeta = 1 - e_{wet}$ , is used as a starting scheme that introduces liquid dissipation into a DEM scheme through  $e_{wet}$ . The force expressions are summarized in figure 1(b) for DEM implementation.

Since the current DEM scheme only calculates the solid sphere motion but neglects the co-existing liquid medium, the total liquid weight is evenly distributed to each particle assuming that the two phases move in coherence. A scale factor,  $\alpha$ , is defined by dividing the liquid mass with the total particle number and used to calculate an 'equivalent' particle mass as  $m_p^* = (1 + \alpha)m_p$  from the original mass,  $m_p$ . After a total force  $F$  is calculated in the soft-sphere contact model with  $m_p$ , the sphere is advanced in DEM with  $F = m_p^* dU/dt$ .

A parallel discrete objects simulation system, called IRIS, has been developed at National Taiwan University (NTU) (Lin, *et al.* [6]) to conduct the current DEM simulation. IRIS is built on VEDO, a C++ framework for discrete object simulation (Yang and Hsieh [7]). The current simulations are conducted on a distributed-memory cluster system with a maximum of 192 nodes (each has 2 HP Integrity RX2600 dual-core processors and 8 gigabyte memory) at Taiwan's National Center for High-Performance Computing (NCHC).

## 3. Preliminary results and future prospects

This DEM scheme is applied to simulate a dry and a wet granulate flow (composed of identical glass spheres) released from stationary in the same flume inclined  $11^\circ$  from the horizontal. A solid-liquid mixture is prepared that matches the total weight of a dry bulk to ensure identical initial potential energy in both systems. Thus,

fewer spheres exist in a wet bulk. Nonetheless, we assume that both systems have sufficient particles to aggregate into a flowing bulk that exhibits a ‘continuum-like’ macroscopic behavior.

### 3.1 The motion and particle distribuion

Figures 2(a)-(b) show a few snapshots on the motion of a dry (2(a)) and a wet (2(b)) mixture—using water at room temperature—after the gate is opened. With the lubricating liquid, the wet mixture moves faster down the flume than a dry bulk. To extrapolate the flow ‘macroscopic’ behavior from the detailed DEM information of the motion of individual sphere, we dissect the whole mixture uniformly into 27 identical averaging boxes,  $3 \times 3 \times 3$  in the  $x$ - $y$ - $z$  flume coordinate system, as illustrated in figure 2(c).

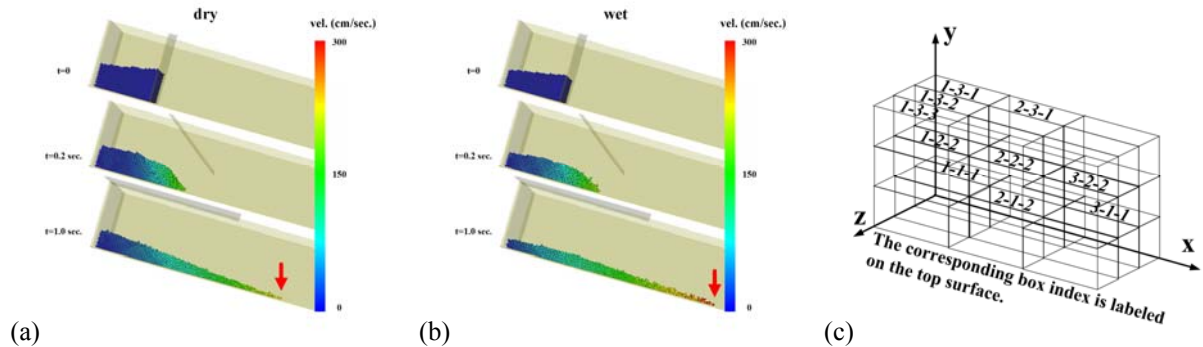


Figure 2: DEM simulation results for the granulate velocity in a (a) dry and (b) wet flow. (c) Structure of the averaging system:  $x$  points downstream,  $y$  is vertical position, and  $z$  denotes span location

The particle distribution within streamwise averaging boxes is first tracked in time and compared in figure 3 at different vertical distances from the base for both dry (3a-b) and wet (3c-d) systems. Once released, the front particles in the 2<sup>nd</sup> vertical front boxes collapse onto the flume base, resulting in sharp decrease of particles—from 150 in 3(b) and 120 in 3(d). This avalanche mechanism explains the consistently increasing or nearly constant number of particles in the basal boxes in 3(a) and 3(c). Furthermore, the interstitial liquid dissipates the kinetic energy of individual particle and somewhat ‘bridges’ the motion of neighboring particles, leading to a more uniform streamwise particle distribution in a wet than in a dry bulk. This phenomenon can be observed when the middle and the rear boxes along the stream, the circle and square lines in 3(c) and (d), are compared to those in 3(a)-(b). Such a bridging effect may also explain why the wet bulk collapses in a manner slower than a dry bulk, which leads to a slower decrease of the particle number in the front boxes (the triangle line) in 3(d) than in 3(b). Due to a narrow flume assigned to the simulation, the flow is rather uniform across the span, as shown by the nearly-matching data along the sidewall and in the middle stream.

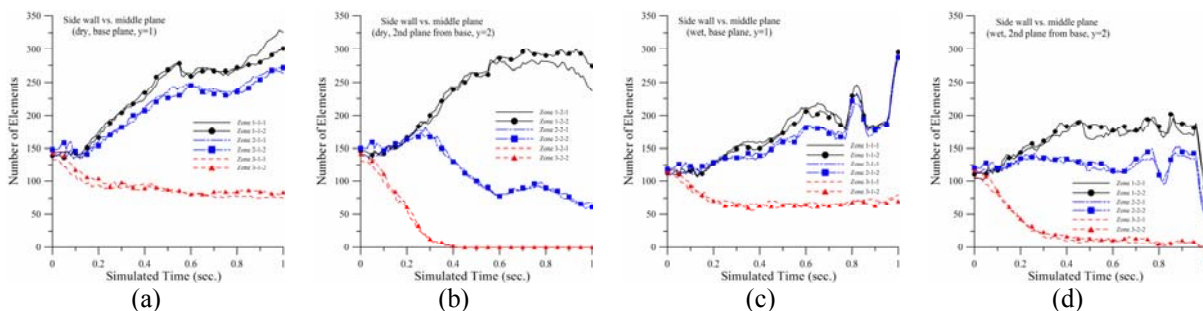


Figure 3: Particle distribution in a dry (a)-(b) and a wet (c)-(d) granular flow at different vertical positions.

### 3.2 The bulk velocity and granular temperature

In figures 4(a) and (b), the average bulk velocity of the streamwise sections are plotted for the dry and the wet granular flows. In both systems, particles in the front accelerates from stationary more rapidly than those stacked in the rear sections. With the lubricating liquids, the wet front particles accelerates at a rate roughly 1.2 times greater than the dry bulk (over the first 0.3 second). The whole mixture asymptotes to a streamwisely uniform acceleration—as indicated by the nearly constant slope—roughly 0.45 second after initiation. This

implies a balance between gravity and the basal friction. Thus, a higher acceleration is found for the wet bulk, about  $120 \text{ cm/s}^2$ , with lubricating liquid than the  $50 \text{ cm/s}^2$  observed in the dry granular flow. In addition, a 'mean' granular temperature (GT) is also calculated to investigate the fluctuation energy in each box and compared for both systems in figures 4(c)-(d) along the stream. Via bridging, the liquid unifies the wet bulk fluctuation energy, from the front to the rear, at around 0.9 sec in figure 4(c); a streamwise gradient in GT is persistent in the dry event. Though GT is of comparable magnitude in both systems, the fluctuation component is less pronounced in a wet bulk motion due to a higher mean bulk translational kinetic energy. This can be also attributed to the liquid bridging and viscous damping effects. Similar unifying liquid effects on GT can also be observed in the middle vertical layer (4(d)).

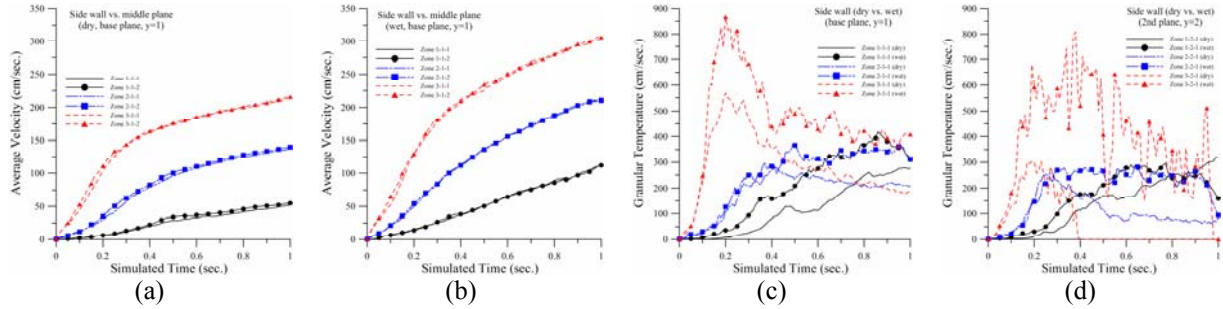


Figure 4: The mean flow behavior: (a)-(b) mean bulk velocity and (c)-(d) granular temperature for dry and wet systems. Granular temperature is calculated by  $GT = \sum_{i=1}^N (U_{i-j} - U_{bulk-j})^2 / 3N$  (Walton and Braun [8]) for the  $N$  particles in each box. The subscript  $j=1-3$  indicates the flow directions.

### 3.3 Prospects and future work

The proposed DEM scheme has been applied successfully to simulate a collision-rich granular flow. With a wet soft-sphere contact model, a solid-liquid mixture exhibits in a faster but less dispersive motion when compared to a dry granular flow, which agrees qualitatively with our preliminary experimental findings. We will conduct further analysis on the simulated and measured data to validate the proposed scheme. In addition, systematic investigations will be performed to reveal the crucial parameters that control the granular bulk mechanics. The granular bulk motion in a wide flume (3x) will also be examined to identify the wall effects, both in DEM simulations and in laboratory experiments. Furthermore, a new model for  $\xi - e_{wet}$  relations may be developed by further examining the interstitial liquid motion.

### References

- [1] Yang FL and Hunt ML, Dynamics of Particle-Particle Collisions in A Viscous Liquid. *Physics of Fluids* 2006; **18**: 121506, 1-11.
- [2] Joseph GG, Zenit R, Hunt ML and Rosenwinkel AM, Particle-Wall Collisions in a Viscous Fluid. *Journal of Fluid Mechanics* 2001; **433**: 329-346.
- [3] Legendre D, Zenit R, Daniel C and Guiraud P. Note on the Modelling of the Bouncing of Spherical Drops or Solid Spheres on A Wall in Viscous Fluid. *Chemical Engineering Science* 2006; **61**: 3543-3549.
- [4] Mindlin RD and Deresiewicz H. Elastic Spheres in Contact under Varying Oblique Forces. *Journal of Applied Mechanics* 1953; **20**: 327-344.
- [5] Cundall PA. Computer Simulations of Dense Sphere Assemblies. In *Micromechanics of Granular Materials*, Satake M and Jenkins JT (eds). Elsevier Science Publishers BV: Amsterdam, 1988; 113-123.
- [6] Lin LS, Hsieh SH and Chang WT, Development of a Parallel Discrete Particle Simulation System for Studying Self-Compacting Concrete Behavior. In *Proceedings of the 11<sup>th</sup> International Conference on Computing in Civil and Building Engineering*, June 14-16, 2006. Montreal, Canada.
- [7] Yang CT and Hsieh SH. An Object-Oriented Framework for Versatile Discrete Objects Using Design Pattern. *Computational Mechanics* 2005; **36** (2): 85-99.
- [8] Walton OR and Braun RL. Viscosity, Granular-Temperature, and Stress Calculations for Shearing Assemblies of Inelastic, Frictional disks. *Journal of Rheology* 1986; **30**(5): 949-980.